A SINGLE MATCHING NETWORK DESIGN FOR A DUAL BAND PIFA ANTENNA VIA SIMPLIFIED REAL FREQUENCY TECHNIQUE

P. Lindberg[1], M. Sengul[2], E. G. Cimen[3], B. S. Yarman[4], A. Rydberg[1], and A. Aksen[3]

[1]*Uppsala University, Box 534, 751 21 Uppsala, Sweden, Email:peter.lindberg@angstrom.uu.se*
[2]*Kadir Has University, P.K. 34083, Fatih, Istanbul, Turkey, Email:msengul@khas.edu.tr*
[3]*Isik University, Kumbaba Mevkii, P.K. 34980, Sile, Istanbul, Turkey, Email:ebrug@isikun.edu.tr, aksen@isikun.edu.tr*
[4]*Tokyo Institute of Technology, Tokyo, Japan, Email:yarman@ec.ss.titech.ac.jp*

ABSTRACT

In this paper, the matched performance of a dual band PIFA antenna is reported. The return loss of the antenna has been optimized over the popular commercial wireless communication bands of 824-960 MHz and 1710-1990 MHz using only one matching network. The network was synthesized using the Simplified Real Frequency Technique, which yields an "easy to implement circuit topology" and realizable component values. With the implemented matching network, a simultaneous measured bandwidth enhancement of 58% and 127% has been achieved in the low and high frequency band, respectively, without significant reduction of radiation efficiency.

Key words: Wireless Communication; Miniaturized Antennas; Wide-Band Matching; PIFA antennas; Dual Band Antennas.

1. INTRODUCTION

With the development of mobile communication systems and miniaturization of hand sets, requirements for compact antennas are rapidly growing. The Planar Inverted F Antenna (PIFA) has found widespread internal utilization within wireless terminals due to its small size for both single [1] and dual band applications [2][3]. The PIFA has many known mechanical advantages, e.g. ease of fabrication, low manufacturing cost, ground plane compatibility and conformity with complex geometries [4]. Concerning electrical properties, it can without difficulty be matched to any impedance (by choosing the location of the short circuit) without matching network, and the design concept is easily extended to dual band functionality [5]. Also, internal PIFA/patch elements have lower SAR (specific absorption rate) values [6] and are less effected (in terms of resonance frequency shift and efficiency reduction) by the presence of the users head in talk position compared to other antennas, e.g. whips/monpoles [7]. Finally, besides improving the matching, the short circuit additionally functions as ESD protection. On the downside, the PIFA typically suffers from a narrow impedance bandwidth, which excludes it from a variety of applications. For example, modern transceiver front-ends are available [8] with quad band support (GSM850/900/1800/1900) for global roaming. Unfortunately, this bandwidth is extremely difficult to achieve with a PIFA within the volume typically allocated for the antenna element. However, it should be kept in mind that without designing a matching network, one would never know what the true realizable bandwidth of the antenna is. Therefore, in this paper, an attempt is made to design a dual band PIFA antenna together with its matching network to asses the achievable antenna performance.

Most research reported on terminal antennas has so far focused on modifications of the radiating element for wide-band [9] and/or multi-band performance [10], as opposed to applying an external matching network. In [11], a microstrip transmission line resonator was integrated with a single-band antenna 900 MHz (patch) element for impedance matching. The concept was extended in [12], where a dual band 900/1800 MHz terminal antenna of similar size as in this paper was matched using an open microstrip stub for extension of the lower band for GSM850/900 coverage. However, the effect on the upper frequency band was a substantial bandwidth reduction.

This paper presents the design and evaluation of a dual band PIFA antenna for the cellular bands GSM900/1800 (890-960 & 1710-1880 MHz). By applying a complex matching network, synthesized using the Simplified Real Frequency Technique (SRFT) [13], the bandwidth of the antenna has been extended for GSM850/900/1800/1900 coverage (824-960 & 1710-1990 MHz). Simulated and measured performance of a prototype antenna is reported.

2. ANTENNA ELEMENT DESIGN

The antenna configuration under consideration is shown in Fig. 1. A flat PIFA element is located in the topmost section 8 mm above a typically sized 35×100 mm^2
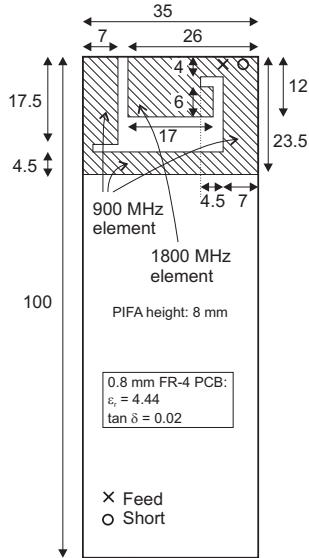
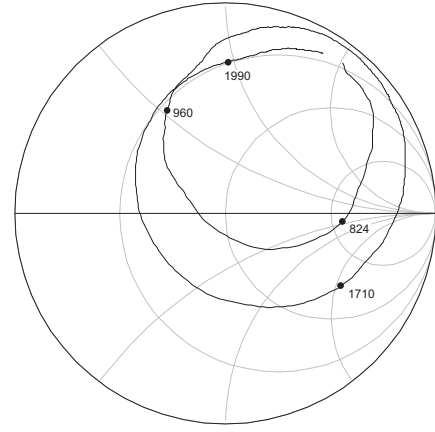*Figure 1. Layout of terminal antenna. All measures in mm.*

Figure 2. Measured impedance (0.7-2.2 GHz) of dual band 900/1800 MHz PIFA. Frequency band limits indicated.
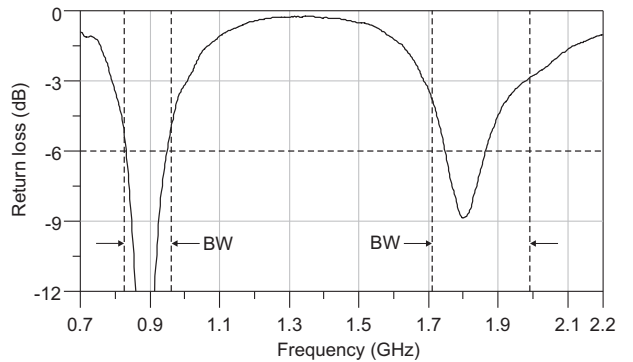

Figure 3. Measured return loss of dual band 900/1800 MHz PIFA without matching network. Frequency limits 824, 960, 1710 and 1990 MHz, together with the typical requirement RL < -6 dB, indicated by dashed lines.

ground-plane, with feeding and short-circuit connected at the top-right positions for maximum impedance bandwidth [14]. Dual-band functionality is implemented by using two unequally sized galvanically coupled resonant patches [5]. A short patch is resonant at 1800 MHz and a longer, bent patch is resonant at 900 MHz, as indicated in Fig. 1. No substrate is used for the PIFA carrier. The chassis is manufactured using single-sided 0.8 mm FR-4 (ϵ_r = 4.44 and $\tan \delta$ = 0.02) PCB, with the bottom side metallized.

The measured input impedance and corresponding return loss (RL) of the PIFA is shown in Fig. 2 and Fig. 3, respectively. As can be seen, the bandwidth (BW) of the radiating element by itself (i.e without matching network) is limited to dual-band coverage of e.g. the GSM900/1800 or GSM850/1900 cellular bands, as is typical for internal antennas of similar size [15][10]. Since the (peak) antenna gain is not interesting for terminal antennas (as directivity is not desired), the 'antenna efficiency', or equivalently 'average gain' becomes the only relevant figure of merit in addition to return loss. The antenna efficiency η_{ant} (i.e. including mismatch losses) was measured in a Satimo STARGATE-64 near-field chamber [16] and is shown in Fig. 4 together with the calculated radiation efficiency $\eta_{rad} = \eta_{ant}/(1 - |\Gamma|^2)$, where Γ is the reflection coefficient at the input terminals and is given from the return loss plot as $|\Gamma| = 10^{(RL/20)}$. The difference between η_{ant} and η_{rad} represents the possible gain increase from perfect impedance matching. In the frequency regions of high return loss, e.g. around 1300 MHz (see Fig. 3), the accuracy of the calculated radiation efficiency is fairly low due to difficulties in measuring exact values of reflection coefficients close to 1. For example, the difference in radiation efficiency for $\Gamma = 0.90$ and $\Gamma = 0.95$ is nearly 3 dB even though $\Delta\Gamma$ is only 0.05. Measured absolute values of antenna efficiency are within ±0.5 dB, with relative values being

significantly more accurate.

It should be noted that the impedance locus in the Smith chart (Fig. 2) is similar for all internal PIFA-type dual-band antennas, fairly independent of the exact geometry of the radiating element. This means that any impedance matching network designed for one antenna is likely to be applicable, with some minor adjustment, to another antenna.

3. MATCHING NETWORK

The impedance matching network was synthesized using the Simplified Real Frequency Technique (SRFT) [13]. The advantages of this technique in practical applications, are

- it utilizes real measured impedance data, as opposed to an equivalent circuit or analytical description of the load impedance function [17][18].
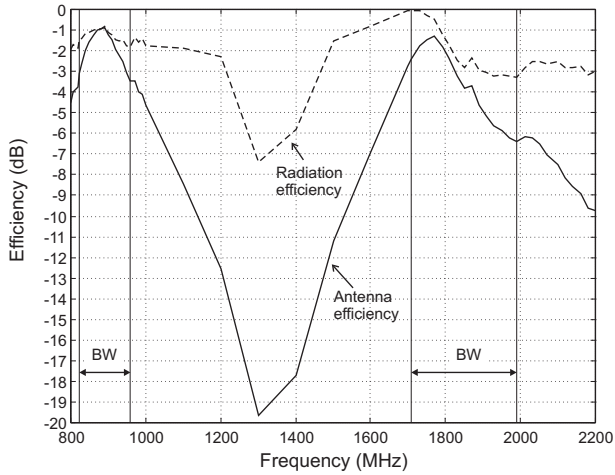
Figure 4. Measured efficiency of PIFA radiator without matching network.

Figure 5. Schematic of matching network from SRFT using measured S-parameters from PIFA element.

Figure 6. Layout of matching network on chassis backside (located in top right corner of Fig. 1).

- it provides the matching network topology, as opposed to simply finding component values in a (by the designer) preselected network.

It should be noted that although analytical theories exists for estimation of achievable gain-bandwidth products [19][17], they are currently limited to simple RC/RLC type load circuits [20]. For real antenna impedances, as indicated in [21], it is almost impossible to asses the gain-bandwidth limitation of the collected data analytically. On the other hand, the Real Frequency Line Segment Technique of Carlin [22] or Simplified Real Frequency Technique provides an insight to matching problems with an excellent estimate for the upper level of the flat transducer power gain, or equivalently the minimum return loss, over the selected frequency bands.

The matching network was implemented using lumped components in preference to distributed transmission lines in order to reduce PCB area consumption. The synthesized network, as shown in Fig. 5, consists of a 7 element low-pass ladder structure. By using a low-pass structure, additional improvements are achieved in terms of harmonic filtering (for power amplifiers in transmitters) and natural absorption of the parasitic reactances of the pads (i.e. shunt capacitance to ground and series inductance from the finite pad lengths) into the component values. The component pads were located coplanar with the ground-plane and arranged so as to minimize the mutual inductance between the coils (as this effect is not included in the schematic optimization) by placing consecutive coils rotated 90°, see Fig. 6. The component values, as given by SRFT using the measured data in Fig. 2, are presented in Tab. 1 under column 'SRFT'. During the implementation of the antenna prototype, one component at a time starting with L1 was mounted on the PCB and the new transformed antenna impedance was measured. As all real components have tolerances in terms of actual inductance/capacitance values, as well as having non-ideal frequency responses due to internal parasitic
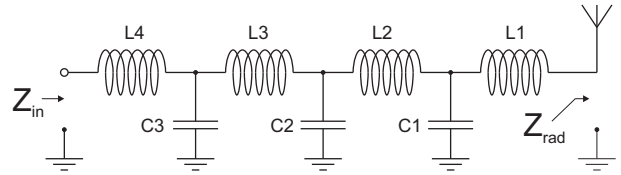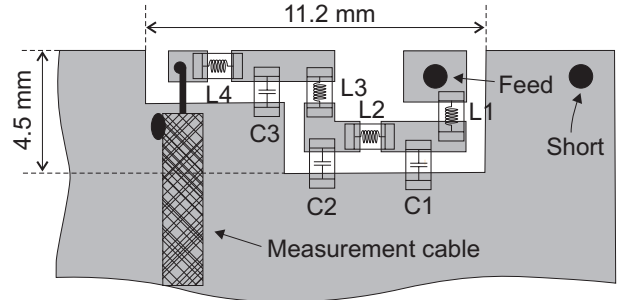
effects (series resistance, inter-winding parallel capacitance of inductors and series inductance of capacitances), a few iterations of component value selection is required for each component. This is also necessary as inductors and capacitors are only available in certain discrete values. After the component which gave the closest measured impedance response compared to the simulated response (using SRFT values) was selected, the remaining network was re-optimized using a standard local gradient method. The final re-optimized values are given in Tab. 1 under column 'Reoptimized'. As can be seen, only minor adjustments were necessary, indicating a good correlation between simulated and measured values of the individual components. The selected component values are located under column 'Actual' in Tab. 1. The inductors used were 0603 high Q $(75 - 120$, depending on frequency and value) components from muRatas LQW18A series with ± 0.5 nH tolerance. The self resonant frequency (due to the inter-winding capacitance) is above 6 GHz for all used values. Maximum DC current through the inductors are 600 mA, with the simulated maximum current amplitude through each inductor displayed in column 'I (mA)' in Tab. 1 with the antenna fed by a +33 dBm 50 Ω source, which is the peak power for GSM850/900 (with 3 dB lower power levels for GSM1800/1900). As typically only one of eight time-slots is used for GSM communication, the given peak currents can be multiplied by $1/8$ and $1/\sqrt{2}$ to obtain the average current through the inductor for comparison with the specified maximum of 600 mA. Clearly, the standard inductors used for the matching network can without difficulty sustain the applied current levels in GSM. The capacitors used were 0505 high Q capacitors from Dielectric Laboratories C11 range, with the first (series) resonance at >5 GHz.

Table 1. *Optimized component values of matching network together with peak current amplitudes through the inductors.*

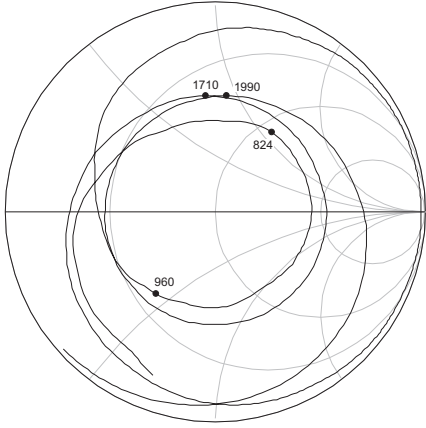| Component	SRFT	Reoptimized	Actual	I (mA)
L1 (nH)	5.17	5.17	7.5	329
C1 (pF)	1.69	1.69	1.2	-
L2 (nH)	11.74	11.79	12	248
C2 (pF)	1.65	1.32	1.2	-
L3 (nH)	12.74	12.79	12	302
C3 (pF)	1.49	1.55	1.5	-
L3 (nH)	5.41	5.66	5.6	259

Figure 7. *Simulated impedance (0.7-2.2 GHz) of antenna with matching network. Frequency band limits indicated.*
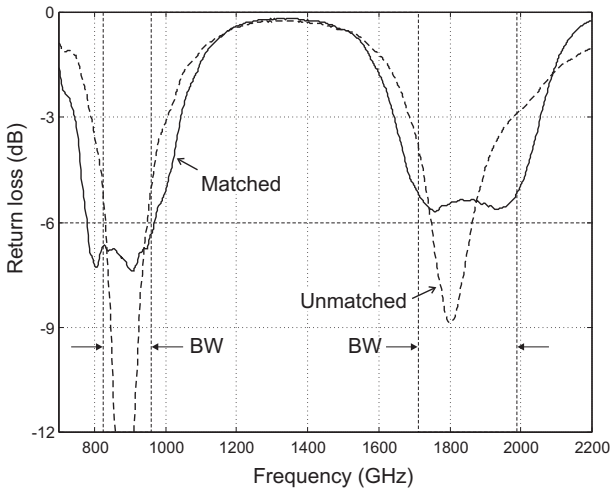

Figure 8. *Simulated return loss of antenna with and without ideal RFT matching network.*

4. RESULTS

The antenna was measured with a coaxial cable connected perpendicular to the chassis length, as shown in Fig. 9. To minimize any influence of the cable on the measurement results (due to the finite size ground plane), the cable was attached at the simulated (using IE3D [23]) E-field minima at 900 MHz, as suggested in [24], which is located approximately at the chassis center in this particular antenna configuration. At 1800 MHz, the chassis is electrically larger and the antenna properties are hence not as sensitive to cable effects compared to at 900 MHz [25]. To further reduce cable effects, a dual band balun was connected to the measurement cable to suppress any induced leakage currents on the outside of the coaxial shield. The balun consists of two series metal L-shaped "fingers" soldered to the coaxial shield, as indicated in Fig. 9. The principle of operation of this balun is identical to the bazooka (or sleeve) balun that has previously been successfully applied during terminal antenna measurements [26] - an unsymmetrical transmission line is formed by the coaxial shield and the metal finger, and by making the finger $L = \lambda/4$ long at the design frequency (900 or 1800 MHz) and connecting the finger to the shield at one end, the short-circuit is transformed into a high-impedance $Z_{in,balun}$ at the open end facing the chassis according to

$$Z_{in,balun} = jZ_0 \tan(\gamma L) \qquad (1)$$

where Z_0 is the characteristic impedance of the transmission line formed by the finger and the coaxial shield, $\gamma = \alpha + j\beta$ is the propagation constant with real part α being the attenuation constant (in Neper/m) and imaginary part β being the phase constant (in rad/m). The high impedance effectively chokes any leakage currents on the shield within a limited bandwidth ($\sim 10\%$) around the design frequency. At the upper frequency band, the first (low band) balun transforms the true short into a virtual short at the open end. However, the second (shorter) balun then connects in series and introduces a virtual open circuit at its open end, again suppressing any radiating currents on the outside of the coaxial shield.

The measured return loss of the matched PIFA is shown in Fig. 10 together with the unmatched return loss as reference. As can be seen, the bandwidth has clearly been enhanced by the implemented matching network, especially at the upper frequency band. As the frequency response is nearly identical to the ideal simulated one, the realizability of implementing SRFT generated matching network for dual band terminal antennas is verified. For the two respective frequency bands, the measured impedance bandwidth (at 6 dB return loss) has been extended from 13.3% to 21.0% in the low band and from 6.3% to 14.3% in the high band, corresponding to a 58% and 127% increase, respectively.

As the addition of lumped components invariably introduces extra losses, the antenna efficiency was remeasured with the matching network applied, as shown
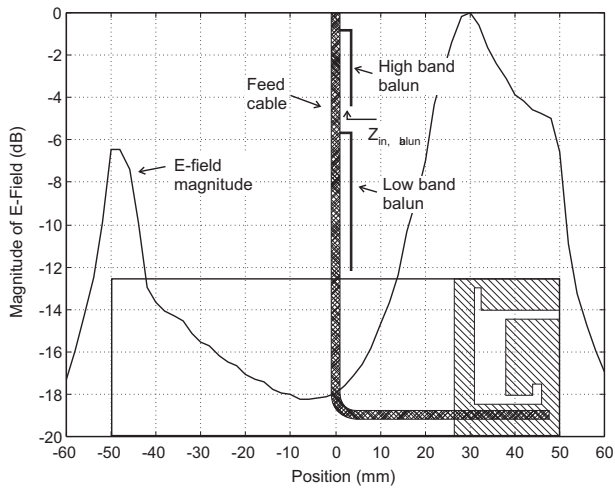
Figure 9. Simulated E-field strength at 900 MHz as a function of chassis position. Placement of measurement cable, together with baluns, is indicated.
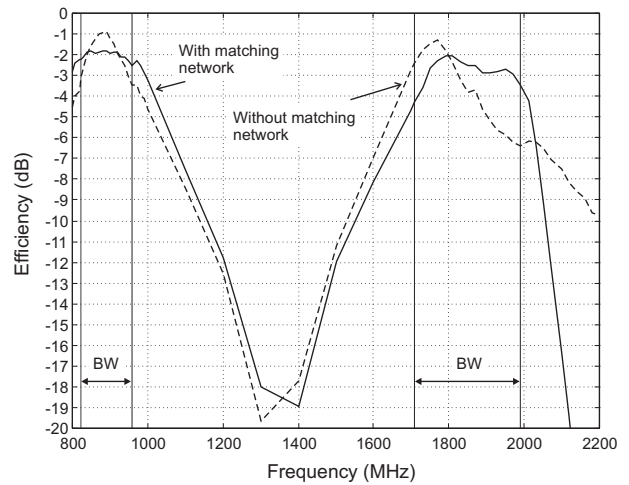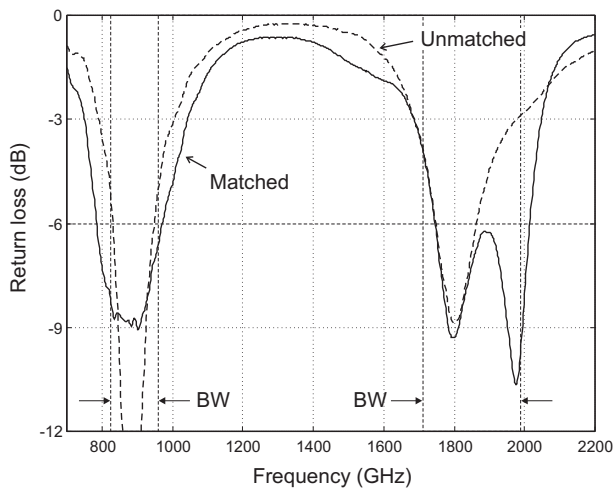

Figure 10. Measured return loss of antenna with and without implemented matching network.

in Fig. 11 together with the antenna efficiency without the matching network as reference. At both frequency bands, the bandwidth enhancement effect on the antenna efficiency is clearly seen. A maximum of 1 dB reduced efficiency compared to the unmatched antenna is seen in the low band, which can be attributed to the near perfect match (RL<-12 dB) (although in a very limited frequency interval) compared to the antenna with the matching network. Hence, the component losses are fairly small at 800-900 MHz. At around 1800 MHz, with nearly identical return loss values, the antenna efficiency is roughly 1 dB lower with the matching network due to component losses.

Figure 11. Measured antenna efficiency of PIFA radiator with and without matching network.

5. CONCLUSIONS

A SRFT synthesized matching network has been implemented and evaluated for enhancing the bandwidth of a standard dual band terminal antenna. Measured results are in close agreement with simulated results using ideal components, validating the method for real practical designs. A bandwidth enhancement factor of 58% and 127% has been achieved at the RL $<$ -6 dB level in the high and low frequency band, respectively, compared to the unmatched antenna.

As the optimum component values given by the SRFT are all fairly small, the network is highly suitable for monolithic on-chip integration, thus enabling small-sized low-cost matching modules. We believe that this kind of module could find widespread application in wide/multiband terminal antenna designs. In particular, as the input impedance of most PIFA elements are typically very similar (reasonably independent of the exact geometry), the matching modules, perhaps from a small library of different variations, could conveniently be used as an ad-hoc solution to already designed antenna elements.

REFERENCES

[1] T. Taga and K. Tsunekawa. Performance analysis of a built-in planar inverted F antenna for 800 MHz

band portable radio units. *IEEE Journal on Selected Areas in Communications*, SAC-5:921–929, June 1987.

[2] C.R. Rowell and R.D. Murch. A compact PIFA suitable for dual-frequency 900/1800-MHz operation. *IEEE Transactions on Antennas and Propagation*, 46(4):596–598, April 1998.

[3] K-L. Wong, Y-C. Lin, and T-C. Tseng. Thin internal GSM/DCS patch antenna for a portable mobile terminal. *IEEE Transactions on Antennas and Propagation*, 54(1):238–242, January 2006.

[4] S. Yarasi, G.R. Kadambi, and T. Hebron. Conformal shaped PIFAs for mobile communication applications. In *Proc. Antennas and Propagation Society International Symposium*, volume 3, pages 82–85, June 2003.

[5] Z.D. Liu, P.S. Hall, and D. Wake. Dual-frequency planar inverted-F antenna. *IEEE Transactions on Antennas and Propagation*, 45(10):1451–1458, October 1997.

[6] G. Lazzi, J. Johnson, S. S. Pattnaik, and O. P. Gandhi. Experimental study on compact, high-gain, low SAR single- and dual-band patch antenna for cellular telephones. In *Proc. Antennas and Propagation Society International Symposium*, volume 1, pages 130–133, June 1998.

[7] K. H. Chan, K. M. Chow, L. C. Fung, and S. W. Leung. SAR of internal antenna in mobile-phone applications. *Microwave and Optical Technologt Letters*, 45(4):286–290, May 2005.

[8] R. Magoon, A. Molnar, J. Zachan, G. Hatcher, and W. Rhee. A single-chip quad-band (850/900/1800/1900 MHz) direct conversion GSM/GPRS RF transceiver with integrated VCOs and fractional-n synthesizer. *IEEE Journal of Solid-State Circuits*, 37(12):1710–1720, December 2002.

[9] K. R. Boyle. Differentially slotted and differentially filled PIFAs. *Electronics Letters*, 39(1):9–10, January 2003.

[10] H-T Chen, K-L. Wong, and T-W. Chiou. Pifa with a meandered and folded patch for the dual-band mobile phone application. *IEEE Transactions on Antennas and Propagation*, 51(9):2468–2471, September 2003.

[11] N. Fayyaz, E. Shin, and S. Safavi-Naeini. A novel dual band patch antenna for GSM band. In *Proc. IEEE AP-S Conference on Antennas and Propagation for Wireless Communications*, pages 156–160, November 1998.

[12] J. Ollikainen, O. Kivekas, C. Ichein, and P. Vainikainen. Internal multiband handset antenna realized with an integrated matching circuit. In *Proc. Antennas and Propagation Society International Symposium*, volume 2, pages 629–632, March 2003.

[13] B. S. Yarman and H. J. Carlin. A simplified real frequency technique applied to broad-band multistage microwave amplifiers. *IEEE Transactions on Microwave Theory and Techniques*, 82:2216–2222, December 1982.

[14] O. Kiveks, J. Ollikainen, T. Lehtiniemi, and P. Vainikainen. Bandwidth, SAR, and efficiency of internal mobile phone antennas. *IEEE Transactions on Electromagnetic Compatibility*, 46(1):71–86, February 2004.

[15] P-L. Teng, S-T. Fang, and K-L. Wong. Pifa with a bent, meandered radiating arm for gsm/dcs dual-band operation. In *Proc. Antennas and Propagation Society International Symposium*, volume 3, pages 107–110, June 2003.

[16] P. O. Iversen, Ph. Garreau, and D. Burrel. Real-time spherical near-field handset antenna measurements. *IEEE Antennas and Propagation Magazine*, 43(3):90–94, June 2001.

[17] R. M. Fano. Theoretical limitations on the broadband matching of arbitrary impedances. *Technical Report*, (41), January 1948.

[18] D. C. Youla. A new theory of broad-band matching. *IEEE Transactions on Circuits and Systems*, 11(1):30–50, March 1964.

[19] H. W. Bode. *Network Analysis and Feedback Amplifier Design*. Van Nostrand, 1945.

[20] K. Yegin and A. Q. Martin. On the design of broad-band loaded wire antennas using the simplified real frequency technique and a genetic algorithm. *IEEE Transactions on Antennas and Propagation*, 51(2):220–228, February 2003.

[21] B. S. Yarman. *Broadband networks - Wiley Encyclopedia of Electrical and Electronics Engineering*, volume 2. Wiley, 1999.

[22] H. J. Carlin. A new approach to gain-bandwidth problems. *IEEE Transactions on Circuits and Systems*, CAS-24(4):170–175, April 1977.

[23] Zeland Software. IE3D v.11, 2005.

[24] P. J. Massey and K. R. Boyle. Controlling the effects of feed cable in small antenna measurements. In *Proc. Antennas and Propagation Society International Symposium*, volume 2, pages 561–564, March 2003.

[25] H. Arai. *Measurement of Mobile Antenna Systems*. Artech House, 2001.

[26] Y. L. Chow, K. F. Tsang, and C. N. Wong. An accurate method to measure the antenna impedance of a portable radio. *Microwave and Optical Technology Letters*, 23(6):349–352, December 1999.